THE JOURNAL OF PHYSICAL CHEMISTRY A

pubs.acs.org/JPCA Article

# Correlation of Photoluminescence and Structural Morphologies at the Individual Nanoparticle Level

*Published as part of The Journal of Physical Chemistry virtual special issue "Time-Resolved Microscopy".*

Luis Gutiérrez-Arzaluz, Ghada H. Ahmed, Haoze Yang, Semen Shikin, Osman M. Bakr, Anton V. Malko,* and Omar F. Mohammed*

Cite This: *J. Phys. Chem. A* 2020, 124, 4855−4860

Read Online

ACCESS | Metrics & More | Article Recommendations

**ABSTRACT:** Single-particle spectroscopy has demonstrated great potential for analyzing the microscopic behavior of various nanoparticles (NPs). However, high-resolution optical imaging of these materials at the nanoscale is still very challenging. Here, we present an experimental setup that combines high sensitivity of time-correlated single-photon counting (TCSPC) techniques with atomic force microscopy (AFM). This system enables single-photon detection with a time resolution of 120 ps and a spatial resolution of 5 nm. We utilize the setup to investigate the photoluminescence (PL) characteristics of both zero-dimensional (0D) and three-dimensional (3D) perovskite nanocrystals and establish a correlation between the particles' sizes, their PL blinking, and the lifetime behavior. Our system demonstrates an unprecedented level of information, opening the door to understanding the morphology−luminescence correlation of various nanosystems.

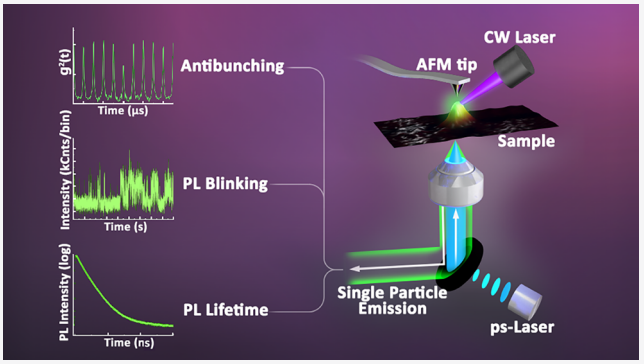


## INTRODUCTION

Since the first demonstrations of single-molecule measurement techniques,[1,2] their rapid progress enabled the discernment of individual features of single nanoparticles (NPs) and provided the direct measurements of their heterogeneity. Optical signatures of individual NPs are often influenced by particle's size, shape, composition, surface states, and the local environments and carry a wealth of information that is obscured in the ensemble measurements. Aided by the rapid advance of ultrasensitive single-photon detectors and time-correlated single-photon counting techniques (TCSPC), photon statistics such as fluorescence blinking, lifetime imaging, and photon antibunching (a measure of the particle's individuality) provide indispensable information about electronic properties of the materials and their underpinning photophysics.[3,4]

Besides all the remarkable information obtained from single-particle optical spectroscopy, a number of limitations exist. The main drawback is the fundamental principle of light diffraction, limiting the resolution between 200 and 300 nm. Super-resolution microscopy techniques,[5,6] while going beyond the diffraction limit, are not readily applicable for single-particle studies in the few nanometer limit. However, transmission (TEM) and scanning (SEM) electron microscopy methods, while possessing requisite nanometer resolution, are difficult to conjugate with the optical properties of individual particles.[7,8] Being in this regime, the plethora of nanomaterials, such as semiconductor quantum dots (QDs), nanocrystals (NCs), and micelles, while extensively studied using single-particle optical spectroscopy methods, have not been correlated with their structural and environmental heterogeneities. Thus, it will be crucial to understand the impact of the size, surface properties, and shape of the particles on their emissive behavior.

Among the nanoscale materials, perovskite nanocrystals (PNCs) have recently attracted considerable interest due to their high emissive properties,[9−12] as well as the straightforward synthetic methods.[10,13,14] Being a relatively new addition to the nanomaterials' field, many open questions still remain, including the microscopic origin of the emissive transitions and the direct influence of particles' shape/size and surface properties. While several papers have researched purely optical emission properties of single three-dimensional (3D) and zero-

Received: March 16, 2020
Revised: April 29, 2020
Published: May 12, 2020

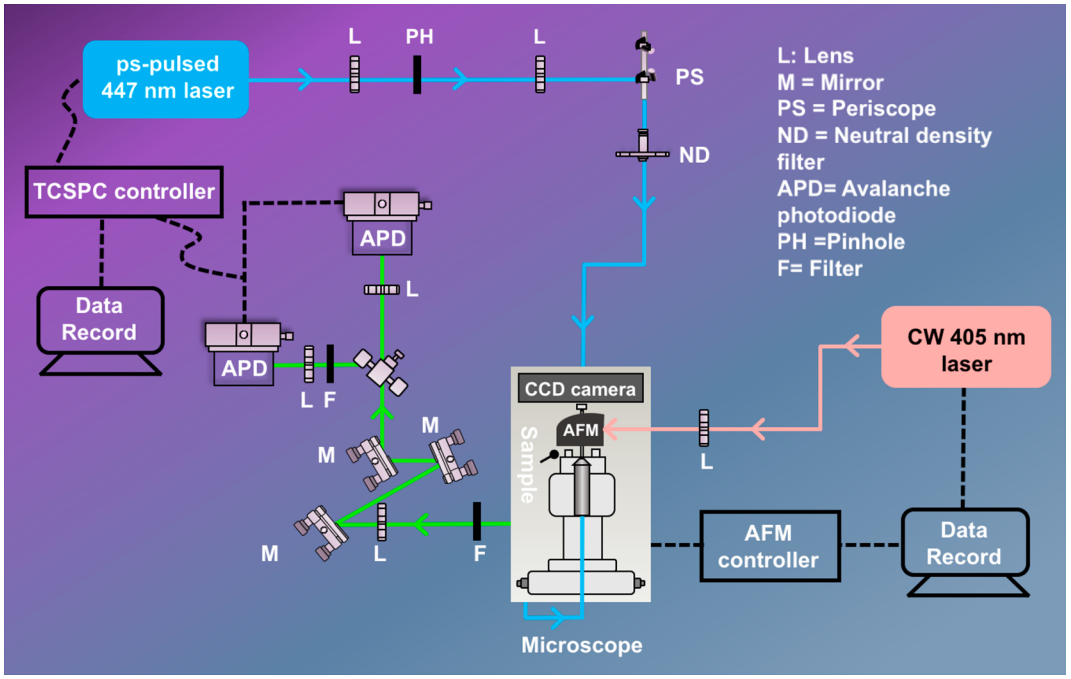


**Figure 1.** Schematic representation of the TCSPC-AFM experimental setup.

dimensional (0D) lead-based PNCs,[9,12,13,15] no attempts have yet been shown to correlate them with the specific structural attributes at the individual particle level.

In this work, we develop an experimental setup that combines TCSPC-based confocal optical detection and atomic force microscopy (AFM) imaging of the same individual PNCs. It has the ability to characterize the topography of the materials at the nanometer resolution while being sufficiently noninvasive to allow extended measurements of time-resolved signatures and statistics of photon correlations. The experimental data for 3D $CsPbBr_3$ and 0D $Cs_4PbBr_6$ PNCs as model systems demonstrate the versatility of the new setup to unveil morphology-luminescence relationships between particles' blinking behavior and size distribution within the inhomogeneously broadened ensemble.

## METHODS

**Synthesis.** For the synthesis of both $Cs_4PbBr_6$ and $CsPbBr_3$ nanocrystals, all reagents were purchased from Sigma-Aldrich and used without any purification. The $Cs_4PbBr_6$ nanocrystals (0D PNCs) were synthesized using a modification of the reported method.[16] First, a mixture of 2.25 g of $Cs_2CO_3$ (99%) and 21.5 mL of oleic acid (90%) was stirred and degassed at 130 °C under vacuum for 1 h to generate a transparent stock of cesium oleate precursor. Then, 0.2 mL of Cs-oleate precursor, 10 mL of anhydrous *n*-hexane (99.98%), and 2 mL of oleic acid were loaded in a 20 mL glass vial. Following that, a well-mixed (by vortex) solution of $PbBr_2$ (0.03 M, DMF, 1 mL), HBr (48 wt %, 15 $\mu$L), 0.1 mL of oleic acid, and 0.05 mL of oleylamine (90%) was swiftly injected into the vial under vigorous stirring. A color change from pale-white to pale-green was observed in 10 min, suggesting the formation of $Cs_4PbBr_6$ nanocrystals. The as-synthesized nanocrystals were collected via centrifugation at 8000 rpm for 5 min. The pellet was finally rinsed with 2 mL of *n*-hexane, followed by dispersion in 2 mL of *n*-hexane for the spectroscopic measurements. The $CsPbBr_3$ nanocrystals (3D PNCs) were synthesized using a similar method as above, except for the usage amount of $PbBr_2$ precursor (0.24 M, DMF, 1 mL) and anhydrous toluene (99.8%) as a solvent.

**Experimental Setup.** In order to achieve single-particle optical characterization and morphological measurements at the nanoscale level, we integrated scanning AFM head into a confocal microscopy system coupled with time-correlated single-photon counting detection. The layout for the system is depicted in Figure 1. The setup consists of three main parts: confocal TCSPC microscope, AFM system, and wide-field microscopy imaging. TCSPC measurements were performed in a modified microscope (Olympus IX71). The excitation source is 447 nm picosecond pulsed laser (70 ps, 100 kHz to 100 MHz variable repetition rate, DeltaDiode, HORIBA) that is passed through a 50 $\mu$m pinhole to clean the laser output mode. The beam is directed to the back-illumination port of the microscope and focused into the sample with a 100×, 1.3 NA oil microscope objective (Olympus). The sample is mounted on the Physik Instrumente (PI) scanning stage that allows sub-50 nm positioning of the individual nanoparticles with respect to the confocal excitation spot. Laser excitation intensity is controlled with a set of neutral density filters (ThorLabs). A wide-field illumination by 405 nm continuous wave (cw) laser (Cobolt 06-MLD) is independently coupled via the top port in the AFM head and allows for the initial particle's localization within the area of interest. A small CCD camera (Thorlabs) with a 405 nm long-pass filter was used to produce real time wide-field images of individual blinking PNCs. To minimize laser exposure, we first performed TCSPC confocal data acquisition on a selected PNC, followed by topographical AFM scanning of the same area to determine the size and shape of the nanoparticle. The scanning AFM head (Smena, NT-MDT) has been mounted on the same PI stage and has its own coarse positioning (25 × 25 mm) and fine scanning (200 × 200 $\mu$m) capabilities. We used Techno-nT VIT_P/IR top visual cantilevers (force constant 25−95 N/m, tip radius 10 nm). The imaging mode was semicontact tapping


https://dx.doi.org/10.1021/acs.jpca.0c02340
J. Phys. Chem. A 2020, 124, 4855−4860

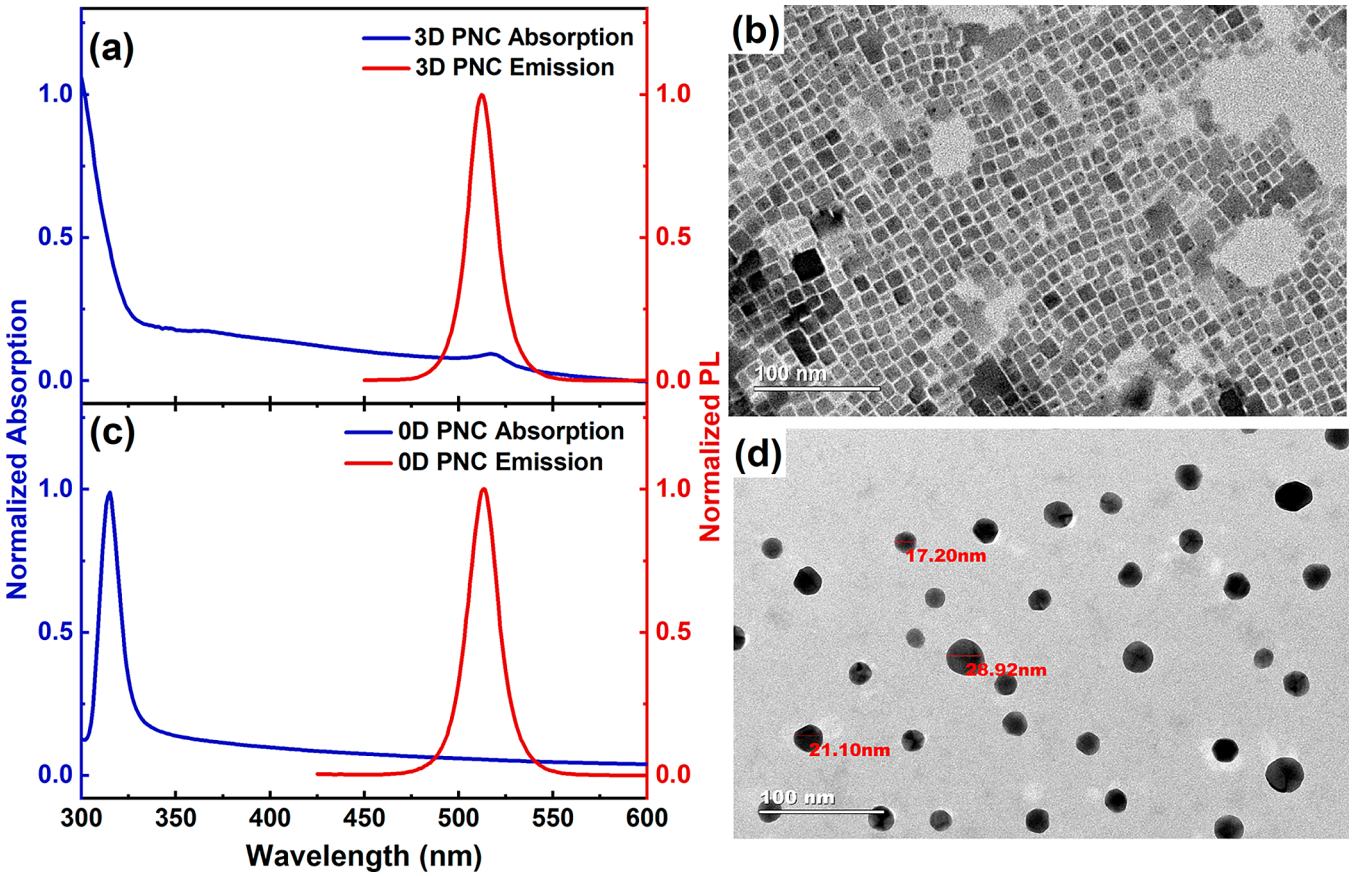


**Figure 2.** Steady-state absorption and photoluminescence for $CsPbBr_3$ (3D) (a) and $Cs_4PbBr_6$ (0D) (c) PNCs in solution, together with TEM images for 3D (b) and 0D (d) nanocrystals.

with 278 kHz oscillation frequency and a set point value of about 6 nA. Typical scanning area is 10 $\mu$m × 10 $\mu$m with 600 × 600 pixels at 0.5 Hz scanning speed. During calibration, the AFM tip was visually aligned to the focal spot of the confocal picosecond laser to ensure both techniques have been measuring the same nanoparticle. All measurements were taken in ambient conditions. During confocal PL detection, the emitted light was filtered with a long-pass 470 nm filter to eliminate scattered laser light. The filtered signal was recollimated and sent into two avalanche photodiodes (APDs, PDM series, Micro Photon Devices) placed in a Hanbury−Brown−Twiss arrangement with a 50/50 beam splitter. Time-tagged TCSPC data was collected using HydraHarp 400 controller (PicoQuant). Photon arrival times were recorded simultaneously, allowing us to compute second-order photon correlation functions. All the lifetime fittings and correlation functions were calculated in SymphoTime 64 software (PicoQuant). For noise-free PL measurements, we first prepared quartz coverslips by cleaning in piranha solution for 1 h and then rinsed with deionized water and methanol. To achieve adequate concentrations for single-particle measurements, stock solutions of $CsPbBr_3$ PNCs were diluted ~100 000 times. After that, ~5 $\mu$L of each dilution was drop-cast on treated quartz slides and dried before performing the experiments.

## RESULTS AND DISCUSSION

The steady-state absorption and photoluminescence spectra and TEM images for 0D and 3D PNCs are presented in Figure 2. For 3D PNCs, Figure 2a shows characteristic absorption and narrow emission spectra at 510 nm. The respective TEM micrograph in Figure 2b indicates that 3D PNCs have a cubic shape and exhibit a range of different sizes from ~10 to ~35 nm within the ensemble. This size distribution confirms that within the sample, particles with different optical properties could be found. However, the 0D PNCs exhibit an emission peak centered at 512 nm (Figure 2c). Also, the TEM image presented in Figure 2d shows spherical particles with a size distribution from ~15 to 40 nm, representing a good agreement with the previously reported data for 0D perovskite nanocrystals.[9,10,16]

Figure 3 demonstrates single-photon emission characteristics and AFM imaging of an individual $Cs_4PbBr_6$ (0D) PNC. The intensity trajectory shown in Figure 3a,b exhibits common blinking behavior characteristic of single emitters like molecular systems and quantum dots.[17−19] The blinking trace presents two well-defined states, the "ON" state with high intensity and the low intensity "OFF" state, characteristic of quenched emission output. We note that emission of the "OFF" state is above the noise level, thus proving the capabilities of the system to detect individual emitters with the low light output. At the same time, the PL emission is split into two detection channels, allowing us to determine the second-order photon correlation function $g^2(\tau)$ simultaneously for the corresponding particle. The $g^2(\tau)$ for the same PNC is shown in Figure 3c. The near absence of the central peak at $\tau$ = 0, known as antibunching (AB), proves the single-photon emitter nature of the emissive transition, demonstrating the capability of our system to perform single-particle measure-


https://dx.doi.org/10.1021/acs.jpca.0c02340
J. Phys. Chem. A 2020, 124, 4855−4860

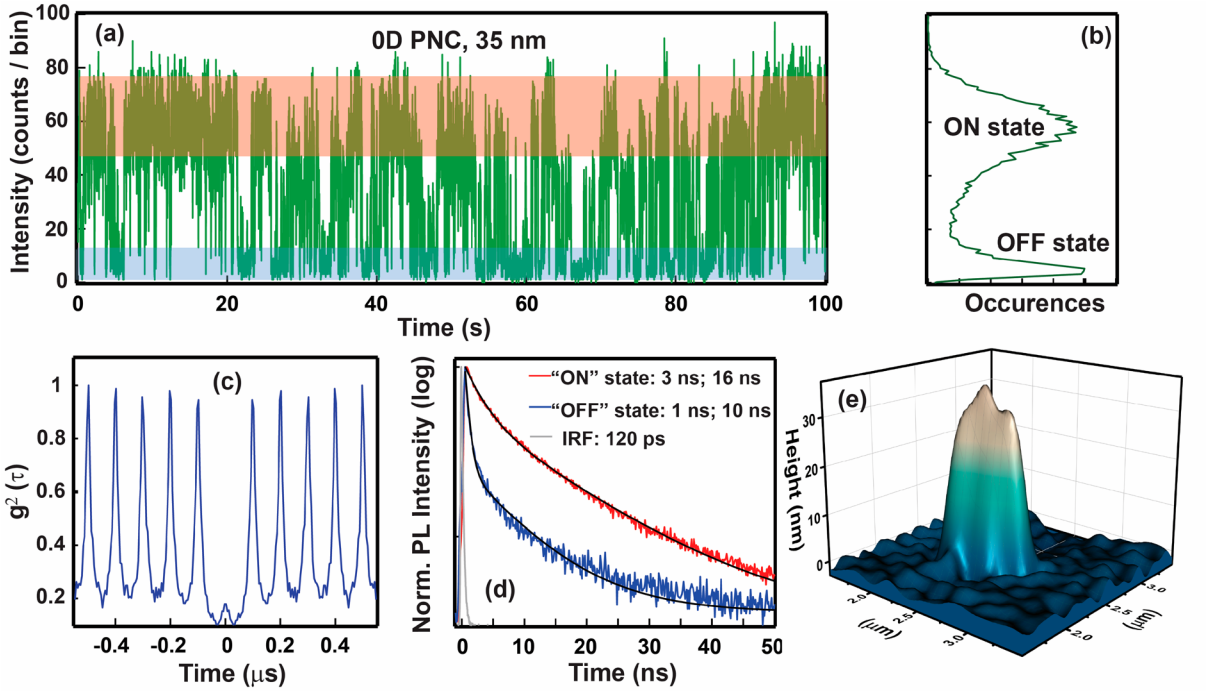


**Figure 3.** Results of $Cs_4PbBr_6$ (0D) PNC measurements from the confocal TCSPC-AFM setup. (a) Blinking trace for a single particle and (b) its occurrence histogram. (c) Photon correlation function, $g^2(\tau)$. (d) Extracted PL decays times, color-coded to bars in (a). PL for the "ON" (red), "OFF" (blue) states and system's IRF (gray). (e) AFM three-dimensional topography of the measured single PNC. Bin size: 20 ms.

ments and discriminate between individual and multiple emitters in the nanocrystals. Using time-tagging TCSPC capabilities, we can process the data to simultaneously extract PL emission lifetimes from any region within the intensity trajectory, thus exploring the nature of the emissive transitions. The PL lifetimes showed in Figure 3d exhibit comparatively long, $\tau_{ON} \sim 16$ ns, PL dynamics of the "ON" state, typical for the excitonic transitions in Cs-based PNCs.[14,20−23] The lifetime of the "OFF" state, $\tau_{OFF} \sim 1-3$ ns, is much shorter. It indicates that the emission is likely coming from a charged (trion) state with the intensity quenched by an Auger-type process.[24] Overall, the confocal, time-tagged TCSPC system is able to resolve PL lifetimes of individual nanoparticles with ∼120 ps time resolution while simultaneously recording two-photon streams to determine photon correlation functions. The longest PL decay collection time window is determined by the laser repetition rate (10 kHz to 100 MHz), allowing us to explore a large variety of chemical and nanomaterial systems.

The surface topography capability of the system is illustrated by the scanning AFM 3D surface reconstruction of the same PNC as displayed in Figure 3e. We found the height of this particle to be about 35 nm, which is in agreement with the typical ensemble average of such 0D perovskite PNCs as recently reported.[14] As the tapping mode of the AFM system has the most sensitivity, the small surface features around the nanoparticle resolved by the AFM allow us to estimate the resolution limit as low as 5 nm. At the same time, the lateral resolution of the system is on the order of 0.2 $\mu$m as can be seen from the lateral extent of the image in Figure 3e. It is worth pointing out that the convolution of the sample morphology with the tip's shape, size, and contact angle determines the lateral size in AFM measurements.[25,26] Since perovskite NCs are "soft" materials, the lateral size convolution can also be affected by the AFM tip "dragging" the particle during the surface scanning. In addition, the ligands capping the PNC's core could spread on the substrate's surface due to capillary forces, further aggravating the lateral size spread. However, the vertical resolution (provided by the "tapping" mode of detection) is not affected by these effects, allowing us to easily differentiate between PNCs of different sizes and shapes within the ensemble.[25]

To correlate a variety of blinking behaviors with particle's size and shape, we have now chosen to explore $CsPbBr_3$ (3D) PNCs. Typically, 3D PNCs have a better size distribution and have been more widely studied compared to 0D ones, thus allowing us to analyze the observed dependencies better. Previous studies have shown that 3D PNCs exhibit shorter PL lifetime compared to the 0D NCs due to the presence of different deactivation pathways for each dimensionality.[15,19,20,27]

Figure 4 exhibits AFM images, blinking traces, and extracted PL lifetimes for three different $CsPbBr_3$ PNCs with heights 8.5, 30, and 45 nm (the last one is at the extreme range of the distribution). All nanoparticles are from the same ensemble with the mean particle size of ∼20 nm. Again, the measured lateral size seems larger due to the material's softness and the tip dimensions mentioned before, but we can observe well-defined boundaries for each nanocrystal. The smallest particle shown in Figure 4a (8.5 nm) exhibits low emission intensity (Figure 4b). The shortest lifetime component of ∼1 ns may indicate that the particle mostly resides in the quenched states, while the longer one, ∼6 ns may indicate the emission from the exciton (Figure 4c). The apparent "noisiness" and the independence of the PL lifetime from the intensity level in this PNC refer to a very quick cycling between the excitonic and the quenched states on a time scale much shorter than the integration bin (20 ms for all blinking traces). Next, for the nanocrystal with ∼30 nm size (Figure 4d), we observe a predominantly "ON" and "OFF" type behavior, with the "ON" states coming in shorter "burst-like" intervals (Figure 4e). The


https://dx.doi.org/10.1021/acs.jpca.0c02340
J. Phys. Chem. A 2020, 124, 4855−4860

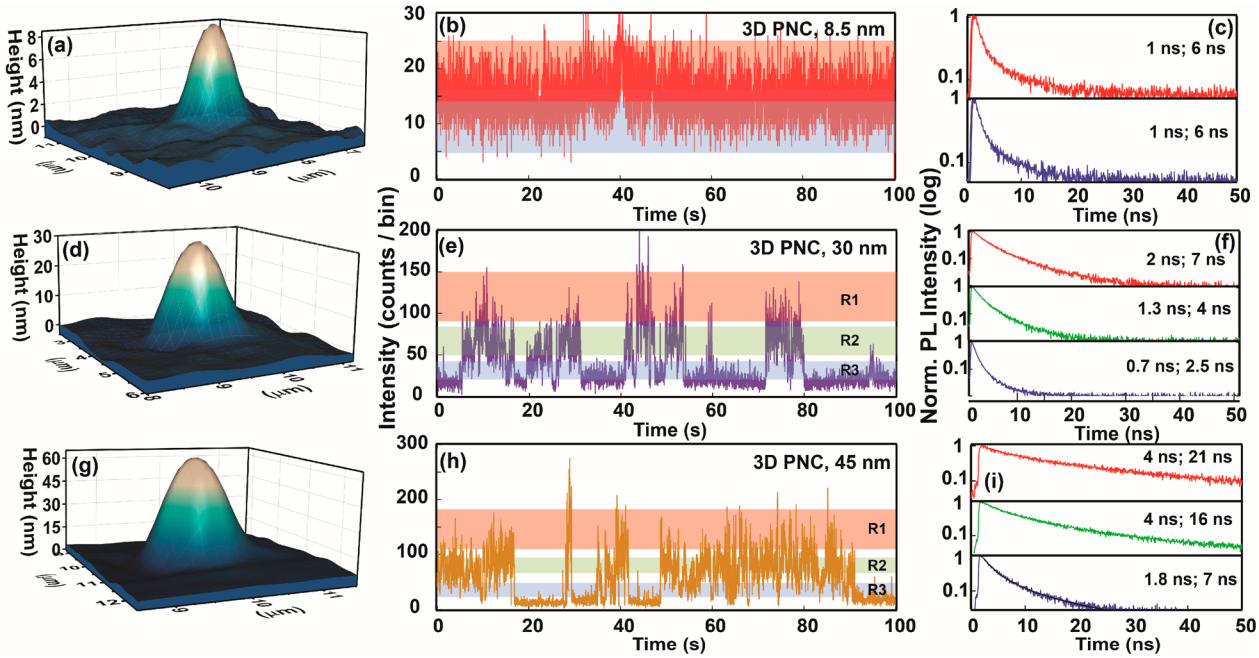


**Figure 4.** Analysis of blinking behavior for $CsPbBr_3$ (3D) PNCs of different sizes. Left column: AFM measurements. Middle column: respective blinking traces, 20 ms bin time. Right column: extracted PL lifetimes, color-coded to the respective intensity cross sections.

PL lifetime cross-sectioning in Figure 4f exhibits several lifetime components, with $\tau_{short} \sim 1-2$ ns and $\tau_{long} \sim 6-7$ ns values. These correspond well with previously measured PL lifetimes for individual 3D PNCs of the similar mean sizes.[20,27] Lastly, the largest nanocrystal (45 nm, Figure 4g) exhibits more of the "bursting" type behavior as well as much longer PL lifetimes as can be observed in Figure 4h, with longer components $\tau_{long} \sim 15-21$ ns (Figure 4i). Such bursting behavior has been recently observed for both 3D and 0D cesium bromide nanocrystals and has been attributed to the emergence of the molecular-like emitters.[14,17,27−29]

This detailed analysis of the relationship between size and single-particle emissive properties has only been made possible by the joint TCSPC-AFM measurements that show a considerable heterogeneity of the optical properties within the ensemble. The difference in sizes allows us to explore different confinement regimes without specifically synthesizing PNCs of different sizes that often present a particular challenge for small size NCs. The observed difference in PL properties could be stemming from the different confinement conditions for the excitons, involvement of various types of excitonic species as well as the emergence of the larger number of localized emissive centers in larger nanoparticles.

## CONCLUSION AND OUTLOOK

In summary, we presented a new setup based on a confocal TCSPC microscope and an AFM system to characterize the photoluminescence from individual nanoemitters. This system offers single-photon detection efficiency of individual nanocrystals combined with high spatial AFM resolution. We demonstrated the broad capabilities of the system by studying (0D and 3D) individual perovskite NCs. We demonstrated that size of the particles directly influences PL lifetime and blinking properties of the perovskite NCs. Further explorations of morphologies and PL emission properties for several types of the PNC emitters are currently underway. This approach could easily be extended to a variety of nanomaterials, from conventional semiconductor NCs to single crystals, heterojunction materials, and thin film embedded molecular systems to give detailed information about how nanoscale morphology affects their luminescent properties.

## AUTHOR INFORMATION


### Corresponding Authors

**Anton V. Malko** − *Department of Physics, The University of Texas at Dallas, Richardson, Texas 75080, United States;* orcid.org/0000-0001-6410-7112; Email: anton.malko@utdallas.edu

**Omar F. Mohammed** − *Division of Physical Sciences and Engineering, King Abdullah University of Science and Technology, Thuwal 23955-6900, Kingdom of Saudi Arabia;* orcid.org/0000-0001-8500-1130; Email: omar.abdelsaboor@kaust.edu.sa

### Authors

**Luis Gutiérrez-Arzaluz** − *Division of Physical Sciences and Engineering, King Abdullah University of Science and Technology, Thuwal 23955-6900, Kingdom of Saudi Arabia*

**Ghada H. Ahmed** − *Division of Physical Sciences and Engineering, King Abdullah University of Science and Technology, Thuwal 23955-6900, Kingdom of Saudi Arabia;* orcid.org/0000-0003-1709-8692

**Haoze Yang** − *Division of Physical Sciences and Engineering, King Abdullah University of Science and Technology, Thuwal 23955-6900, Kingdom of Saudi Arabia*

**Semen Shikin** − *Division of Physical Sciences and Engineering, King Abdullah University of Science and Technology, Thuwal 23955-6900, Kingdom of Saudi Arabia*

**Osman M. Bakr** − *Division of Physical Sciences and Engineering, King Abdullah University of Science and Technology, Thuwal 23955-6900, Kingdom of Saudi Arabia;* orcid.org/0000-0002-3428-1002

Complete contact information is available at: https://pubs.acs.org/10.1021/acs.jpca.0c02340




https://dx.doi.org/10.1021/acs.jpca.0c02340
J. Phys. Chem. A 2020, 124, 4855−4860

### Notes

The authors declare no competing financial interest.

## ■ ACKNOWLEDGMENTS

The authors gratefully acknowledge financial support from King Abdullah University of Science and Technology (KAUST).

## ■ REFERENCES

(1) Moerner, W. E.; Kador, L. Optical Detection and Spectroscopy of Single Molecules in a Solid. *Phys. Rev. Lett.* **1989**, *62*, 2535−2538.
(2) Orrit, M.; Bernard, J. Single Pentacene Molecules Detected by Fluorescence Excitation in a p-Terphenyl Crystal. *Phys. Rev. Lett.* **1990**, *65*, 2716−2719.
(3) Frantsuzov, P.; Kuno, M.; Janko, B.; Marcus, R. A. Universal Emission Intermittency in Quantum Dots, Nanorods and Nanowires. *Nat. Phys.* **2008**, *4*, 519−522.
(4) Sampat, S.; Karan, N. S.; Guo, T.; Htoon, H.; Hollingsworth, J. A.; Malko, A. V. Multistate Blinking and Scaling of Recombination Rates in Individual Silica-Coated CdSe/CdS Nanocrystals. *ACS Photonics* **2015**, *2*, 1505−1512.
(5) Lesyuk, R.; Cai, B.; Reuter, U.; Gaponik, N.; Popovych, D.; Lesnyak, V. Quantum-Dot-in-Polymer Composites via Advanced Surface Engineering. *Small Methods* **2017**, *1*, 1700189.
(6) Jin, D.; Xi, P.; Wang, B.; Zhang, L.; Enderlein, J.; van Oijen, A. M. Nanoparticles for Super-resolution Microscopy and Single-Molecule Tracking. *Nat. Methods* **2018**, *15*, 415−423.
(7) Koberling, F.; Mews, A.; Philipp, G.; Kolb, U.; Potapova, I.; Burghard, M.; Basché, T. Fluorescence Spectroscopy and Transmission Electron Microscopy of the Same Isolated Semiconductor Nanocrystals. *Appl. Phys. Lett.* **2002**, *81*, 1116−1118.
(8) Orfield, N. J.; McBride, J. R.; Keene, J. D.; Davis, L. M.; Rosenthal, S. J. Correlation of Atomic Structure and Photoluminescence of the Same Quantum Dot: Pinpointing Surface and Internal Defects that Inhibit photoluminescence. *ACS Nano* **2015**, *9*, 831−839.
(9) Riesen, N.; Lockrey, M.; Badek, K.; Riesen, H. On the Origins of the Green Luminescence in the "Zero-Dimensional Perovskite" $Cs_4PbBr_6$: Conclusive from Results Cathodoluminescence Imaging. *Nanoscale* **2019**, *11*, 3925−3932.
(10) Tang, X.; Chen, W.; Liu, Z.; Du, J.; Yao, Z.; Huang, Y.; Chen, C.; Yang, Z.; Shi, T.; Hu, W.; et al. Ultrathin, Core-Shell Structured $SiO_2$ Coated $Mn^{(2+)}$ -Doped Perovskite Quantum Dots for Bright White Light-Emitting Diodes. *Small* **2019**, *15*, No. e1900484.
(11) Yin, J.; Yang, H.; Song, K.; El-Zohry, A. M.; Han, Y.; Bakr, O. M.; Bredas, J. L.; Mohammed, O. F. Point Defects and Green Emission in Zero-Dimensional Perovskites. *J. Phys. Chem. Lett.* **2018**, *9*, 5490−5495.
(12) Yu, H.; Wang, H.; Zhang, J.; Lu, J.; Yuan, Z.; Xu, W.; Hultman, L.; Bakulin, A. A.; Friend, R. H.; Wang, J.; et al. Efficient and Tunable Electroluminescence from *in Situ* Synthesized Perovskite Quantum Dots. *Small* **2019**, *15*, No. e1804947.
(13) Chen, K.; Schunemann, S.; Song, S.; Tuysuz, H. Structural Effects on Optoelectronic Properties of Halide Perovskites. *Chem. Soc. Rev.* **2018**, *47*, 7045−7077.
(14) Zhang, Y.; Guo, T.; Yang, H.; Bose, R.; Liu, L.; Yin, J.; Han, Y.; Bakr, O. M.; Mohammed, O. F.; Malko, A. V. Emergence of Multiple Fluorophores in Individual Cesium Lead Bromide Nanocrystals. *Nat. Commun.* **2019**, *10*, 2930.
(15) Chen, Q.; Wu, J.; Ou, X.; Huang, B.; Almutlaq, J.; Zhumekenov, A. A.; Guan, X.; Han, S.; Liang, L.; Yi, Z.; et al. All-Inorganic Perovskite Nanocrystal Scintillators. *Nature* **2018**, *561*, 88−93.
(16) Yang, H.; Zhang, Y.; Pan, J.; Yin, J.; Bakr, O. M.; Mohammed, O. F. Room-Temperature Engineering of All-Inorganic Perovskite Nanocrsytals with Different Dimensionalities. *Chem. Mater.* **2017**, *29*, 8978−8982.
(17) Barak, Y.; Meir, I.; Shapiro, A.; Jang, Y.; Lifshitz, E. Fundamental Properties in Colloidal Quantum Dots. *Adv. Mater.* **2018**, *30*, No. e1801442.
(18) Cordones, A. A.; Leone, S. R. Mechanisms for Charge Trapping in Single Semiconductor Nanocrystals Probed by Fluorescence Blinking. *Chem. Soc. Rev.* **2013**, *42*, 3209−21.
(19) Saidaminov, M. I.; Almutlaq, J.; Sarmah, S.; Dursun, I.; Zhumekenov, A. A.; Begum, R.; Pan, J.; Cho, N.; Mohammed, O. F.; Bakr, O. M. Pure $Cs_4PbBr_6$: Highly Luminescent Zero-Dimensional Perovskite Solids. *ACS Energy Lett.* **2016**, *1*, 840−845.
(20) Yarita, N.; Tahara, H.; Ihara, T.; Kawawaki, T.; Sato, R.; Saruyama, M.; Teranishi, T.; Kanemitsu, Y. Dynamics of Charged Excitons and Biexcitons in $CsPbBr_3$ Perovskite Nanocrystals Revealed by Femtosecond Transient-Absorption and Single-Dot Luminescence Spectroscopy. *J. Phys. Chem. Lett.* **2017**, *8*, 1413−1418.
(21) Muhammed, M. M.; Mokkath, J. H. Electric Field Hotspots of All-Inorganic Off-Stoichiometric $APbX_3$ (A = Cs, Rb and X = Cl, Br, I) Perovskite Quantum Dots. *Phys. E* **2019**, *113*, 65−71.
(22) Lekina, Y.; Shen, Z. X. Excitonic States and Structural Stability in Two-Dimensional Hybrid Organic-Inorganic Perovskites. *J. Sci.: Adv. Mater. Devices* **2019**, *4*, 189−200.
(23) Seth, S.; Samanta, A. Photoluminescence of Zero-Dimensional Perovskites and Perovskite-Related Materials. *J. Phys. Chem. Lett.* **2018**, *9*, 176−183.
(24) Makarov, N. S.; Guo, S.; Isaienko, O.; Liu, W.; Robel, I.; Klimov, V. I. Spectral and Dynamical Properties of Single Excitons, Biexcitons, and Trions in Cesium−Lead-Halide Perovskite Quantum Dots. *Nano Lett.* **2016**, *16*, 2349−2362.
(25) Voigtländer, B., Static Atomic Force Microscopy. In *Atomic Force Microscopy*; Springer, 2019; pp 199−208.
(26) Schietinger, S.; Aichele, T.; Wang, H. Q.; Nann, T.; Benson, O. Plasmon-Enhanced Upconversion in Single $NaYF_4$:$Yb^{3+}$/$Er^{3+}$ Co-doped Nanocrystals. *Nano Lett.* **2010**, *10*, 134−8.
(27) Guo, T.; Bose, R.; Zhou, X.; Gartstein, Y. N.; Yang, H.; Kwon, S.; Kim, M. J.; Lutfullin, M.; Sinatra, L.; Gereige, I.; et al. Delayed Photoluminescence and Modified Blinking Statistics in Alumina-Encapsulated Zero-Dimensional Inorganic Perovskite Nanocrystals. *J. Phys. Chem. Lett.* **2019**, *10*, 6780−6787.
(28) Yin, J.; Maity, P.; De Bastiani, M.; Dursun, I.; Bakr, O. M.; Bredas, J. L.; Mohammed, O. F. Molecular Behavior of Zero-Dimensional Perovskites. *Sci. Adv.* **2017**, *3*, No. e1701793.
(29) Efros, A. L.; Nesbitt, D. J. Origin and control of blinking in quantum dots. *Nat. Nanotechnol.* **2016**, *11*, 661−71.


https://dx.doi.org/10.1021/acs.jpca.0c02340
J. Phys. Chem. A 2020, 124, 4855−4860